Journal of chemical & engineering data

pubs.acs.org/jced Article

N_2O Solubility in and Density and Viscosity of Novel Biphasic Solvents for CO_2 and Their Phase Separation Accelerators from 293.15 to 333.15 K

Mimi Xu, Shujuan Wang,* and Lizhen Xu

Cite This: *J. Chem. Eng. Data* 2020, 65, 598−608 Read Online

ACCESS | Metrics & More | Article Recommendations | Supporting Information

ABSTRACT: Densities and viscosities of aqueous solutions of monoethanolamine (MEA)−diethylene glycol dimethyl ether (DGM), MEA−sulfolane (TMS), diethylenetriamine (DETA)−DGM, DETA−TMS, DETA−dimethyl sulfoxide (DMSO), and their phase separation accelerators DGM, DMSO, and TMS aqueous solutions were studied from 293.15 to 333.15 K. N_2O solubilities in MEA−DGM, MEA−TMS, DETA−DGM, DETA−TMS, and DETA−DMSO solutions were measured from 313.15 to 333.15 K. The experiments cover the mole fraction ranges (0−13.5 mol %) DGM, (0−8.92 mol %) DMSO, (0−9.93 mol %) TMS, (14.22−23.12 mol %) MEA + (0−9.63 mol %) DGM, (4.25−7.26 mol %) DETA + (0−10.88 mol %) DGM, (5.68−9.06 mol %) DETA + (0−14.49 mol %) TMS, (11.21−18.21 mol %) MEA + (0−14.57 mol %) TMS, and (5.68−7.42 mol %) DETA + (0−11.87 mol %) DMSO in mixed solutions. Experimental data were correlated well with empirical equations from literature studies which are a function of the temperature and the concentrations of amines and physical solvents.

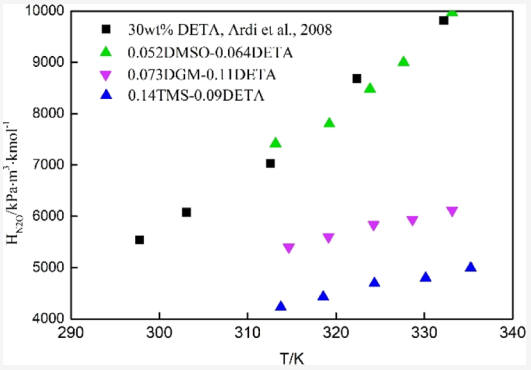

1. INTRODUCTION

Amine scrubbing is considered as the most potential technology to mitigate the greenhouse gas CO_2 emissions because of its adaptability and uncomplicated application in power stations.[1] Aqueous monoethanolamine (MEA), diethanolamine (DEA), and piperazine solutions have been studied in CO_2 capture.[2−4] Energy penalty and cost reduction improvements are needed in this process and one way of reducing the regeneration cost is by using phase splitting solvents.[5] In recent years, there is a growing interest in liquid−liquid biphasic solvents for CO_2 absorption. Raynal et al.[6] proposed a novel biphasic process system DMX using lipophilic solvents and the energy penalty was estimated to be 2.3 GJ/t CO_2. Diethylamino-ethanol (DEEA) and 1,4-butanediamine (BDA) blends, *N*-methyl-1,3-diaminopropane and DEEA blends, dimethylcyclohexylamine and DEEA mixtures, and some other solvents were studied for the biphasic system.[7−10]

In our previous paper, 21 pairs of chemical−physical blends were found to be potential biphasic solvents with much better comprehensive absorption capacity than 30 wt % MEA.[11] Diethylene glycol dimethyl ether (DGM), MEA−sulfolane (TMS), and dimethyl sulfoxide (DMSO) were chosen as phase separation accelerators, and MEA, diethylenetriamine (DETA) and BDA were the main absorption solvents. Results showed that the solvent solution split into two liquid phases when loading sufficient amount of CO_2, and much more CO_2 was enriched in the rich phase rather than in the lean phase. The regeneration energy was estimated to be lower than traditional solvents, and therefore, the basic properties of these solvents should be measured before further study.

Physicochemical properties of solvents are fundamental data in the process modeling and design of gas treatment equipment. Density is required to calculate the physical solubility of CO_2 in solvents, mass transfer, and kinetics parameters. Viscosity data is fundamental for the estimation of the kinetics properties and mass transfer using the modified Stock−Einstein equation.[12] The physical solubility of CO_2 in aqueous solutions are essential to the modeling of thermodynamics and kinetics. However, there is no direct way to detect the physical solubility of CO_2 in aqueous amine solutions because CO_2 reacts with amines spontaneously. A "N_2O analogy" method was proposed in order to calculate the physical dissolving characteristics of CO_2 indirectly in amine systems, and it was verified by Laddha et al.[13−15] The CO_2 molecule and N_2O molecule are similar in molecular configuration and electronic structure, and N_2O does not react with amines and thus physical solubility of CO_2 in the solvents could be calculated indirectly, as shown in eq 1.

Received: August 21, 2019
Accepted: January 10, 2020
Published: January 21, 2020

$$H_{CO_2\text{-s}} = \left(\frac{H_{CO_2\text{-w}}}{H_{N_2O\text{-w}}}\right) H_{N_2O\text{-s}} \quad (1)$$

where $H_{CO_2\text{-s}}$ and $H_{N_2O\text{-s}}$ are the Henry's constants of CO_2 and N_2O in solvents, respectively, Pa·m^3·mol^{-1}. $H_{CO_2\text{-w}}$ and $H_{N_2O\text{-w}}$ are the Henry's constants of CO_2 and N_2O in water studied by Monteiro and Svendsen.[16] As published by Monteiro, accurate Henry's constant correlations of CO_2 and N_2O in water are essential when using the equation of N_2O analogy, and the latest modeling results with 95% confidence bands were given.

Our previous study shows that MEA and DETA were potential amines for liquid−liquid biphasic solvents for their higher cyclic capacity and lower toxicity.[11] Also, DGM, DMSO, and TMS were much more favorable phase separation accelerators than *n*-propanol for their high boiling point. Therefore, the following five kinds of chemical−physical biphasic solvents were studied in this work: MEA−DGM, MEA−TMS, DETA−DGM, DETA−TMS, and DETA−DMSO because MEA−DMSO did not split into two liquid phases after loading CO_2.

At present, there are some comprehensive experiments in which the density of and viscosity in MEA or DETA solutions were measured.[17−19] However, the existing studies on the physical property of DGM, DMSO, and TMS aqueous solutions were inadequate[20−25] with the limited experimental temperatures and solvent concentrations, and the data should be extended. Besides, literature studies on the physicochemical properties of MEA−DGM, MEA−TMS, DETA−DGM, DETA−TMS, and DETA−DMSO aqueous solutions can hardly be found so far.

The purpose of this work is to report the experimental data of density and viscosity of (0−13.5 mol %) DGM, (0−8.92 mol %) DMSO, and (0−9.93 mol %) TMS solution (293.15−333.15 K), and the density, viscosity of and N_2O solubility in MEA−DGM, MEA−TMS, DETA−DGM, DETA−TMS, and DETA−DMSO aqueous blends (293.15−333.15 K). Three semiempirical equations were used to correlate the experimental data on density, viscosity, and N_2O solubility as functions of solvent content and temperature.

Table 1. Chemicals Used in the Experiment

chemical	CAS registry number	source	purity[a]
MEA	141-43-5	Macklin Company	≥99.38 wt %
DETA	111-40-0	Macklin Company	≥99.31 wt %
DGM	111-96-6	Macklin Company	≥99.50 wt %
DMSO	67-68-5	Macklin Company	≥99.16 wt %
TMS	126-33-0	Macklin Company	≥99.93 wt %
N_2O	10024-97-2	Air Liquide Company	≥99.99 mol %
CO_2	124-38-9	Air Liquide Company	≥99.99 mol %

[a]The purities were provided by the suppliers.

2. EXPERIMENTAL SECTION

2.1. Chemicals. Chemicals shown in Table 1 are used as it is, and deionized water was used to prepare experimental solutions.

2.2. Density and Viscosity. A KEM DA640 densimeter with an accuracy of 0.0001 g·cm^{-3} was used to measure the solution density automatically at the specific temperature. Each sample was detected three times to minimize deviations and the average of three repeated tests was accepted. The accuracy of this densimeter was verified by comparing the density of MEA and H_2O with references as shown in Table 2; the data fit well with that in the refs 26−29.

A viscometer (A&D SV-10) was used to measure the viscosity with a given accuracy of ±1% in the range of 0.3−1000 mPa·s. As shown in Figure 1, the H_2O viscosity was measured to calibrate the viscometer and the data from this work agree well with that in the literature studies.[7,17,30]

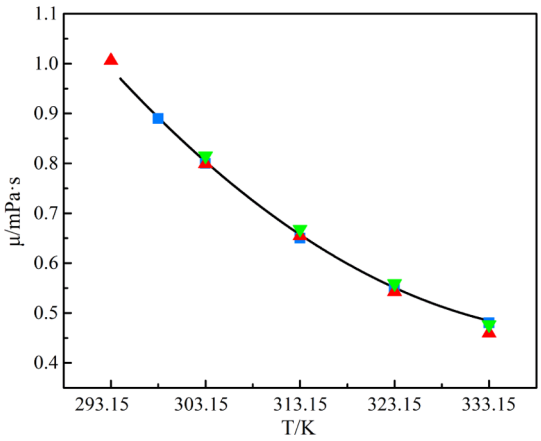

Figure 1. H_2O viscosity from this work and other literature studies from 293.15 to 333.15 K at p = 101 kPa. Green ▼, ref 27; red ▲, ref 17; blue ■, ref 7; and black solid line, this work.

2.3. Physical Solubility of N_2O. The physical solubility of N_2O in aqueous solutions was studied using a self-established

Table 2. Comparison for Density ρ of H_2O and MEA between Experimental and Literature Data (293.15−333.15 K, p = 101 kPa)[a]

		ρ/g·cm^{-3}						
	T/K	experiment	ref	deviation (%)	ref	deviation (%)	ref	deviation (%)
H_2O	293.15	0.9982	0.998204	0.00				
	303.15	0.9957	0.995647	0.01	0.996	0.03	0.9956	−0.01
	313.15	0.9922	0.992215	0.00	0.992	−0.02	0.9922	0.00
	323.15	0.9882	0.988037	0.02			0.9880	−0.02
	333.15	0.9832	0.9832	0.00			0.9832	0.00
MEA	303.15	1.0079	1.0098	−0.19	1.0091	0.12	1.0098	0.19
	308.15	1.0039	1.0048	−0.09				
	313.15	0.9998	1.0009	−0.11	1.0013	0.15	1.0009	0.11
	323.15	0.9921	0.9929	−0.08	0.9934	0.13	0.9929	0.08
	333.15	0.9838	0.9849	−0.11	0.9854	0.16	0.9849	0.11

[a]Standard uncertainties: $u(p)$ = 1 kPa, $u(T)$ = 0.1 K, and $u(\rho)$ = 0.001 g·cm^{-3}.

https://dx.doi.org/10.1021/acs.jced.9b00806
J. Chem. Eng. Data 2020, 65, 598−608

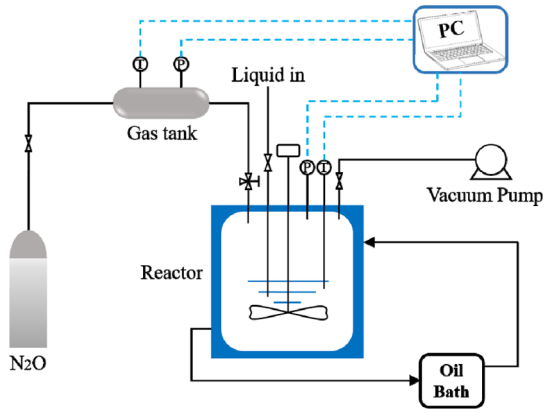

Figure 2. N_2O solubility apparatus.

solubility apparatus shown in Figure 2, which was modified from the report of Wang et al.[7] The apparatus has two principle parts: a glass reactor (2.186×10^{-3} m^3) which is made of quartz with a low coefficient of heat expansion and a stainless steel gas tank (2.63×10^{-4} m^3). See a detailed description of the structure and the theory of this apparatus in the report by Xu et al.[7]

A certain mass of aqueous solution was injected into a glass reactor, and then the reactor was evacuated using a vacuum pump. Then, the stirrer was set at 400 rpm and the water bath was turned on at a specific temperature. The reactor was cut off from the atmosphere with good sealing, and it took 4−6 h (depending on temperature) for the establishment of vapor−liquid equilibrium. A certain amount of N_2O was then added to the reactor from the gas tank by quickly turning on the gas check between the gas tank and reactor. In order to minimize the vapor loss during the experiment, the air tightness of the apparatus was tested and a one-way valve was installed between the gas tank and the reactor to prevent the vapor from leaking back into the gas tank when injecting. During the experiment, the water bath was controlled at a specific temperature which was not totally equal to the solution temperature inside the reactor because of the heat radiation of the reactor and pipes. The temperature inside the reactor and gas tank were recorded by K-type thermocouples with an uncertainty of ±0.1 K, and two pressure sensors were used to record the pressure of the gas tank and the reactor with uncertainty 0.5% of full scale (600 kPa) in the whole process.

The molar quantity of adding N_2O in the reactor, $n^{add}_{N_2O}$, was calculated by the Peng−Robinson (P−R) equation as a function of initial and equilibrium state parameters as shown in eq 2.

$$n^{add}_{N_2O} = \frac{V_t}{R}\left(\frac{P_{V1}}{T_{V1}Z_1} - \frac{P_{V2}}{T_{V2}Z_2}\right) \quad (2)$$

where P_{V1} and P_{V2} are the gas tank pressure before and after injection, Pa; T_{V1} and T_{V2} are the tank temperature before and after injection, K; Z_1 and Z_2 are the compressibility factor of gas before and after injection; R is the universal gas constant, 8.3145 J/(mol·K); and V_t is the gas tank volume, m^3. In the vapor−liquid equilibrium state of the reactor, the amount of N_2O in the gas phase, $n^{g}_{N_2O}$, was obtained from the equilibrium partial pressure of N_2O with the P−R formula as shown in eq 3.

$$n^{g}_{N_2O} = \frac{P_{N_2O}(V_r - V_l)}{z_{N_2O}RT_r} \quad (3)$$

where T_r is the equilibrium reactor temperature, K; z_{N_2O} is the compressibility factor of N_2O at the equilibrium state. P_{N_2O} is the N_2O equilibrium partial pressure in the reactor, Pa; V_r is the reactor volume, m^3; and V_l is the added solvent volume, m^3.

Then, the molar quantity of N_2O dissolved in solvent was calculated with eq 4.

$$n^{l}_{N_2O} = n^{add}_{N_2O} - n^{g}_{N_2O} \quad (4)$$

The N_2O content in the solution, C_{N_2O}, can be worked out with eq 5.

$$C^{l}_{N_2O} = \frac{n^{l}_{N_2O}}{V_s} \quad (5)$$

Then, the Henry's constant of N_2O which stands for the solubility can be expressed as given in eq 6.

$$P_{N_2O} = H_{N_2O} \cdot C^{l}_{N_2O} \quad (6)$$

Before studying solvents, the N_2O solubility in deionized water from 298 to 343 K was measured to verify the apparatus. The experimental results show good consistency to other researchers' data with an average deviation of 0.63% (Figure 3).[31−33]

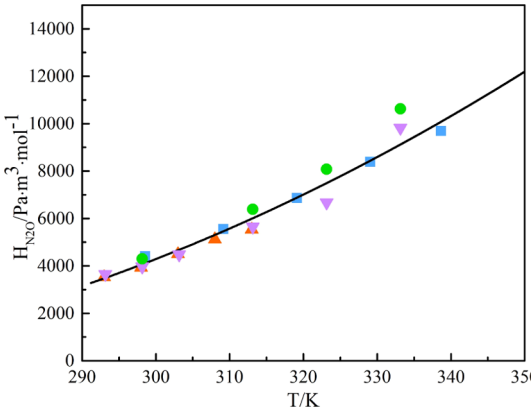

Figure 3. Henry's law constant H_{N_2O} of N_2O in water. Purple ▼, ref 7; orange ▲, ref 28; blue ■, this work; black solid line, ref 16; and green ●, ref 33.

3. RESULTS AND DISCUSSION

3.1. Density. The experimental density results of DGM, TMS, and DMSO aqueous solutions are given in Figures 4−7 and Table 3.

The densities of TMS and DMSO solutions were observed to decrease with increasing temperature or decreasing concentration. As for DGM solution, the densities decrease with the increase of temperature; however, along with the DGM concentration increasing, the densities increase first and then decrease. Because there are few reference data in the range of concentration and temperature used in this study, only some density data about TMS aqueous solution were compared here as shown in Figure 6.[34−36]

The experimental result in this work is consistent with that in refs 34 and 35 which indicates that the experimental result in this study is reliable. As for the data from ref 36, the average deviation between this work and ref 36 is 1% which is a bit higher than that of the refs 34 and 35, but the deviation is acceptable because the

https://dx.doi.org/10.1021/acs.jced.9b00806
J. Chem. Eng. Data 2020, 65, 598−608

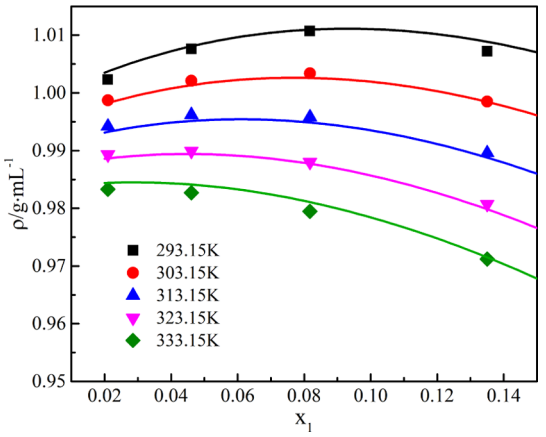

Figure 4. Densities with mole fraction x_1 of aqueous DGM solutions in this work. Markers, experimental result; solid lines, calculated in this work.

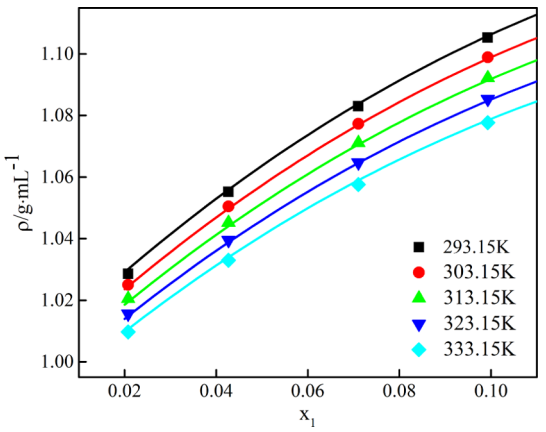

Figure 5. Densities with mole fraction x_1 of aqueous TMS solutions in this work. Markers, experimental result; solid lines, calculated in this work.

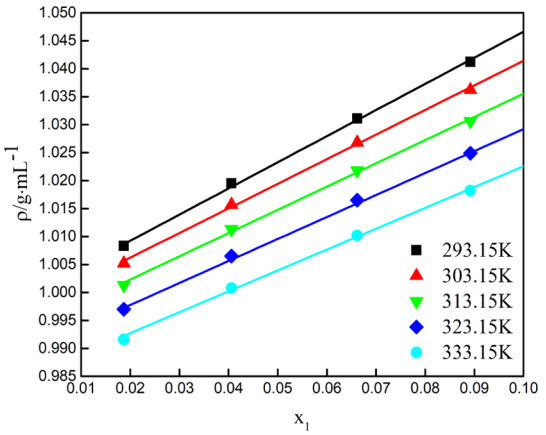

Figure 6. Densities with mole fraction x_1 of aqueous DMSO solutions in this work. Markers, experimental result; solid lines, calculated in this work. The $10x_1/10x_2$ (mol/mol) are 1.422/0, 1.831/0.455, 2.045/0.682, and 2.312/0.963 for black ■, red ●, blue ▲, and pink ▼, respectively.

data from ref 35 were calculated by a regression equation rather than the real experimental data. The experimental data were fitted with eq 7 which takes the temperature and the mole fraction of solvents as independent variable.[37]

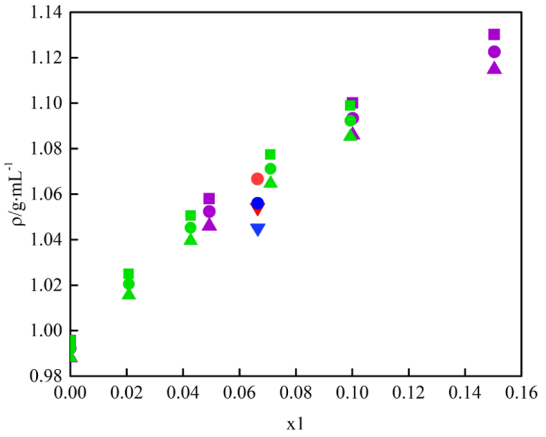

Figure 7. Comparation of densities of aqueous TMS solutions between references and this work. Purple ■, ●, and ▲, 303.15, 313.15, and 323.15 K, respectively, ref 34; green ■, ●, and ▲, 303.15, 313.15, and 323.15 K, respectively, this work; red ● and ▼, 313.45 and 333.55 K, respectively, ref 35; blue ● and ▼, 313.45 and 333.55 K, respectively, ref 36.

Table 3. Densities ρ of DGM, TMS, and DMSO (Mole Fraction of Physical Solvents x_1) Aqueous Solutions at Various Temperatures at p = 101 kPa[a]

	density, $\rho \times 10^{-3}$ (kg·m^{-3})				
	DGM, $10x_1$ (mol/mol)				
T/K	0	0.2100	0.4611	0.8173	1.3503
293.15	0.9982	1.0023	1.0076	1.0107	1.0072
303.15	0.9957	0.9987	1.0021	1.0034	0.9985
313.15	0.9922	0.9942	0.9962	0.9958	0.9896
323.15	0.9882	0.9893	0.9899	0.9880	0.9807
333.15	0.9832	0.9833	0.9827	0.9795	0.9712
	density, $\rho \times 10^{-3}$ (kg·m^{-3})				
	TMS, $10x_1$ (mol/mol)				
T/K	0	0.2077	0.4267	0.7103	0.9929
293.15	0.9982	1.0286	1.0552	1.0830	1.1053
303.15	0.9957	1.0250	1.0505	1.0773	1.0989
313.15	0.9922	1.0205	1.0452	1.0711	1.0922
323.15	0.9882	1.0156	1.0395	1.0647	1.0853
333.15	0.9832	1.0097	1.0330	1.0576	1.0777
	density, $\rho \times 10^{-3}$ (kg·m^{-3})				
	DMSO, $10x_1$ (mol/mol)				
T/K	0	0.1869	0.4060	0.6619	0.8921
293.15	0.9982	1.0083	1.0195	1.0311	1.0412
303.15	0.9957	1.0052	1.0157	1.0268	1.0362
313.15	0.9922	1.0013	1.0113	1.0218	1.0306
323.15	0.9882	0.9970	1.0065	1.0165	1.0249
333.15	0.9832	0.9916	1.0008	1.0102	1.0182

[a]Standard uncertainties are $u(x_1)$ = 0.0002, $u(T)$ = 0.1 K, $u(p)$ = 1 kPa, and $u(\rho)$ = 0.001 g·cm^{-3}.

$$\rho_{\mathrm{ps-amine}} = \left[k_1 + \frac{k_2}{T}(x_{\mathrm{ps}} + k_3 x_{\mathrm{amine}}) + \frac{k_4}{T^2}\right] \times \exp\left[\frac{k_5}{T} + k_6(x_{\mathrm{ps}} + k_3 x_{\mathrm{amine}})\right] \quad (7)$$

where $\rho_{\mathrm{ps-amine}}$ is the density of the blends, 10^{-3} (kg·m^{-3}); T is the experimental temperature, K; and x_{ps} and x_{amine} is the mole fraction of physical solvents and amine, respectively.

https://dx.doi.org/10.1021/acs.jced.9b00806
J. Chem. Eng. Data 2020, 65, 598−608

Table 4. Fitted Factors, AADs, and R^2 for Densities of DGM, DMSO, and TMS Solutions

	k_1	k_2	k_3	k_4	k_5	k_6	AAD[a]	R^2[b]
DGM	0.9237	547.57	119,140	4780.57	5.67	−1.6206	8.23×10^{-4}	0.9919
TMS	1.1485	1873.69	45,981.40	66,211.51	−190.51	−1.8833	7.25×10^{-4}	0.9991
DMSO	0.6346	66.39	138,016.35	−14,103.15	221.01	−0.0135	3.92×10^{-4}	0.9990

[a]AAD = $(1/N)\sum_{i=1}^{N}((|\rho_{cal,i} - \rho_{exp,i}|)/\rho_{exp,i})$. [b]The squared correlation coefficients.

Table 5. Densities of Aqueous MEA−DGM, DETA−DGM, DETA−TMS, MEA−TMS, and DETA−DMSO (Mole Fraction of Amines x_1, Mole Fraction of Physical Solvents x_2) Blended Solutions from 293.15 to 333.15 K at p = 101 kPa[a,b]

		density, $\rho \times 10^{-3}$ (kg·m^{-3})				
		T/K				
solvent	$10x_1/10x_2$ (mol/mol)	293.15	303.15	313.15	323.15	333.15
MEA−DGM	1.422/0	1.0160	1.0114	1.0060	1.0005	0.9942
	1.831/0.455	1.0215	1.0144	1.0070	0.9996	0.9916
	2.045/0.682	1.0196	1.0123	1.0043	0.9963	0.9880
	2.312/0.963	1.0160	1.0076	0.9992	0.9909	0.9820
DETA−DGM	0.425/0	1.0073	1.0035	0.999	0.9943	0.9885
	0.604/0.627	1.0193	1.0117	1.0037	0.9957	0.9871
	0.637/0.795	1.0184	1.0101	1.0017	0.9933	0.9844
	0.726/1.088	1.015	1.0063	0.9974	0.9887	0.9793
DETA−TMS	0.568/0	1.0113	1.0069	1.0019	0.9968	0.9908
	0.696/0.560	1.0673	1.0608	1.0540	1.0471	1.0395
	0.813/1.061	1.1009	1.0934	1.0856	1.0779	1.0696
	0.906/1.449	1.1184	1.1107	1.1028	1.0950	1.0865
MEA−TMS	1.121/0	1.0126	1.0082	1.0033	0.9981	0.9921
	1.390/0.554	1.0681	1.0616	1.0550	1.0483	1.0408
	1.578/0.944	1.0940	1.0869	1.0796	1.0722	1.0642
	1.821/1.457	1.1184	1.1107	1.1028	1.0950	1.0865
DETA−DMSO	0.568/0	1.0113	1.0069	1.0019	0.9968	0.9908
	0.642/0.519	1.0360	1.0300	1.0236	1.0172	1.0100
	0.688/0.826	1.0474	1.0407	1.0336	1.0266	1.0187
	0.742/1.187	1.0580	1.0506	1.0429	1.0351	1.0267

[a]The x_1 and x_2 are the mole fractions of amine and physical solvents, respectively. [b]Standard uncertainties: $u(x_1)$ = 0.0002, $u(x_2)$ = 0.0002, $u(T)$ = 0.1 K, and $u(\rho)$ = 0.001 g·cm^{-3}.

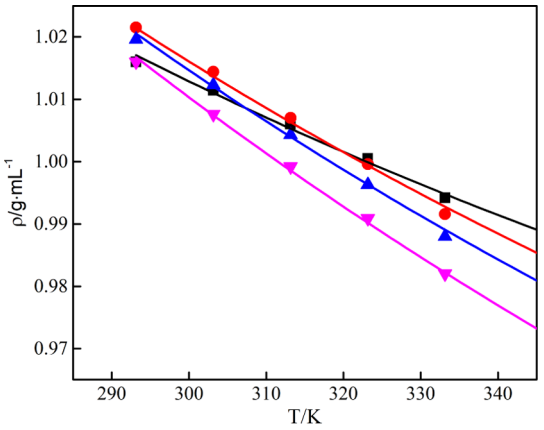

Figure 8. Density results of aqueous MEA−DGM solutions in this work. The $10x_1/10x_2$ (mol/mol) are 1.422/0, 1.831/0.455, 2.045/0.682, and 2.312/0.963 for black ■, red ●, blue ▲, and pink ▼, respectively. Solid lines, calculated in this work.

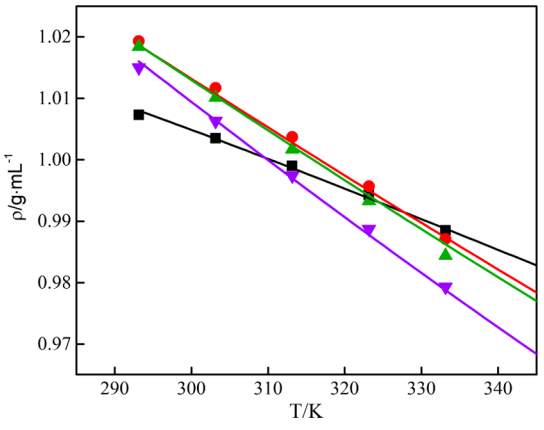

Figure 9. Density results of aqueous DETA−DGM solutions in this work. The $10x_1/10x_2$ (mol/mol) are 0.425/0, 0.604/0.627, 0.637/0.795, and 0.726/1.088 for black ■, red ●, green ▲, and purple ▼, respectively. Solid lines, calculated in this work.

k_1−k_6 are constant factors fitted from the experimental data. The calculated factors k, the average absolute deviations (AADs), and the squared correlation coefficients (R^2) are given in Table 4.

Figures 4−6 show that the results calculated with eq 7 are consistent with experimental results in this study. Besides, the squared correlation coefficients (R^2) are all higher than 0.99 for DGM, DMSO, and TMS solutions.

Further, the densities of five chemical−physical biphasic solvents (MEA−DGM, DETA−DGM, DETA−TMS, MEA−TMS, and DETA−DMSO) were measured from 293.15 to 333.15 K as shown in Table 5 and Figures 8−12.

https://dx.doi.org/10.1021/acs.jced.9b00806
J. Chem. Eng. Data 2020, 65, 598−608

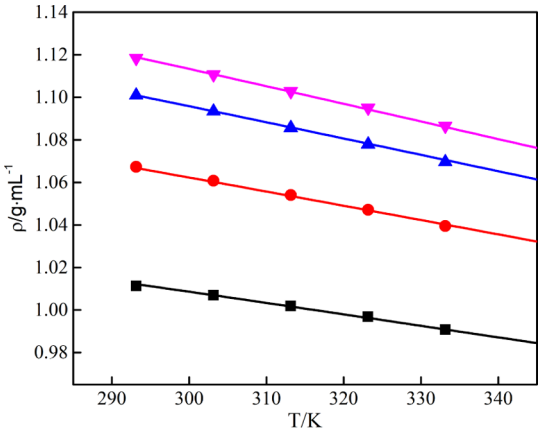

Figure 10. Density results of aqueous DETA−TMS solutions in this work. The $10x_1/10x_2$ (mol/mol) are 0.568/0, 0.696/0.560, 0.813/1.061, and 0.906/1.449 for black ■, red ●, blue ▲, and pink ▼, respectively. Solid lines, calculated in this work.

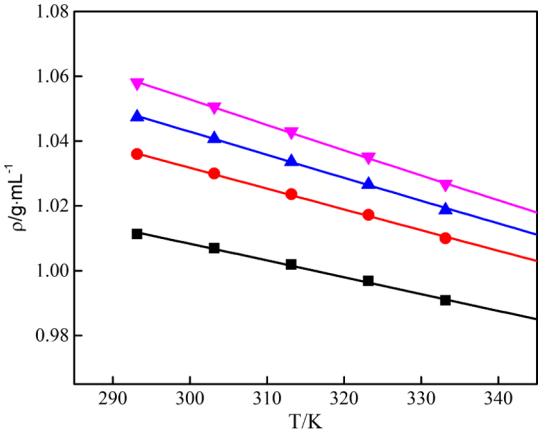

Figure 11. Density results of aqueous DETA−DMSO solutions in this work. The $10x_1/10x_2$ (mol/mol) are 0.568/0, 0.642/0.519, 0.688/0.826, and 0.742/1.187 for black ■, red ●, blue ▲, and pink ▼, respectively. Solid lines, calculated in this work.

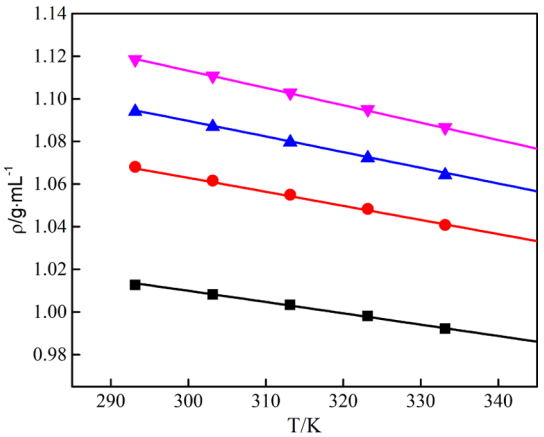

Figure 12. Density results of aqueous MEA−TMS solutions in this work. The $10x_1/10x_2$ (mol/mol) are 1.121/0, 1.390/0.554, 1.578/0.944, and 1.821/1.457 for black ■, red ●, blue ▲, and pink ▼, respectively. Solid lines, calculated in this work.

As shown in Figures 8 and 9, densities decrease faster with increasing temperature when adding DGM to MEA and DETA solution. The blends with higher DGM mole fraction show lower densities at certain temperatures. The Figures 10−12 show that densities increase with the addition of TMS or DMSO to DETA or MEA solutions at the same temperature. The solutions which contain higher TMS or DMSO mole fraction have higher densities.

Table 6. Viscosities of DGM, TMS, and DMSO (Mole Fraction of Physical Solvents x_1) Aqueous Solutions at Various Temperatures at p = 101 kPa[a]

	viscosity, μ (mPa·s)				
	DGM, $10x_1$ (mol/mol)				
T/K	0	0.2100	0.4611	0.8173	1.3503
298.15	0.89	1.36	2.03	2.84	3.11
303.15	0.80	1.19	1.71	2.35	2.62
313.15	0.65	0.94	1.27	1.75	1.93
323.15	0.56	0.78	1.01	1.34	1.46
333.15	0.48	0.65	0.86	1.07	1.17
	viscosity, μ (mPa·s)				
	TMS, $10x_1$ (mol/mol)				
T/K	0	0.2077	0.4267	0.7103	0.9929
298.15	0.89	1.01	1.17	1.59	1.64
303.15	0.80	0.91	1.04	1.34	1.44
313.15	0.65	0.74	0.84	1.01	1.15
323.15	0.56	0.63	0.70	0.84	0.96
333.15	0.48	0.58	0.63	0.75	0.83
	viscosity, μ (mPa·s)				
	DMSO, $10x_1$ (mol/mol)				
T/K	0	0.1869	0.4060	0.6619	0.8921
298.15	0.89	1.01	1.19	1.44	1.69
303.15	0.80	0.91	1.05	1.27	1.48
313.15	0.65	0.73	0.85	1.00	1.15
323.15	0.56	0.62	0.71	0.84	0.96
333.15	0.48	0.55	0.60	0.72	0.78

[a]Standard uncertainty: $u(x_1)$ = 0.0002, $u(T)$ = 0.1 K, $u(p)$ = 1 kPa, and the relative standard uncertainty is $u_r(\mu)$ = 0.15.

3.2. Viscosity. The measurement results and correlation parameters of DGM, TMS, DMSO, MEA−DGM, DETA−DGM, DETA−TMS, MEA−TMS, and DETA−DMSO solutions are given in Tables 6−8 and Figures 13−20. The viscosities of binary and ternary blends go up when the mole fraction of physical solvents was increased or the temperature was decreased. The viscosity results were fitted with eq 8 which takes temperature and concentration of amines and physical solvents as independent variables.[37]

$$\mu_{ps+amine} = \left[1 + k_1\frac{(x_{amine} + k_2x_{ps})}{T} + k_3\frac{(x_{amine} + k_2x_{ps})^2}{T^2}\right] \times \exp\left[\frac{k_4}{T} + \frac{k_5}{T^2} + k_6(x_{amine} + k_2x_{ps})^2\right] \quad (8)$$

where $\mu_{ps+amine}$ is the viscosity of physical solvents and amine blends, mPa·s; x_{amine} and x_{ps} are mole fractions of amines and physical solvents, respectively; T is the temperature, K; and k_1−k_6 are the fitted factors. As shown in Figures 13−20, the viscosities calculated with eq 8 are consistent with the experimental results which indicates that the empirical equation is practical.

3.3. Solubility of N_2O. The solubilities of N_2O in MEA−DGM, DETA−DGM, DETA−TMS, MEA−TMS, and DETA−DMSO solutions are presented in Figures 21 and 22,

https://dx.doi.org/10.1021/acs.jced.9b00806
J. Chem. Eng. Data 2020, 65, 598−608

Table 7. Viscosities of Aqueous MEA−DGM, DETA−DGM, DETA−TMS, MEA−TMS, and DETA−DMSO (Mole Fraction of Amines x_1, Mole Fraction of Physical Solvents x_2) Blended Solutions from 298.15 to 333.15 K at p = 101 kPa[a]

		viscosity, μ (mPa·s)				
		T/K				
solvent	$10x_1/10x_2$ (mol/mol)	298.15	303.15	313.15	323.15	333.15
MEA−DGM	1.422/0	3.11	2.65	1.99	1.55	1.23
	1.831/0.455	5.96	4.87	3.30	2.40	1.85
	2.045/0.682	6.56	5.34	3.68	2.69	2.02
	2.312/0.963	6.85	5.61	3.83	2.79	2.12
DETA−DGM	0.425/0	2.44	2.06	1.55	1.23	0.99
	0.604/0.627	6.66	5.28	3.55	2.54	1.92
	0.637/0.795	6.88	5.48	3.64	2.61	1.97
	0.726/1.088	7.86	6.26	4.15	2.88	2.15
DETA−TMS	0.568/0	3.46	2.88	2.07	1.60	1.26
	0.696/0.560	5.57	4.52	3.15	2.33	1.80
	0.813/1.061	7.75	6.29	4.29	3.10	2.34
	0.906/1.449	9.30	7.48	5.08	3.64	2.73
MEA−TMS	1.121/0	2.44	2.09	1.59	1.27	1.01
	1.390/0.554	3.76	3.17	2.35	1.82	1.42
	1.578/0.944	4.57	3.87	2.84	2.16	1.69
	1.821/1.457	5.72	4.81	3.53	2.60	2.02
DETA−DMSO	0.568/0	3.46	2.88	2.07	1.60	1.26
	0.642/0.519	5.69	4.64	3.24	2.36	1.78
	0.688/0.826	7.04	5.69	3.84	2.72	2.05
	0.742/1.187	8.30	6.64	4.35	3.06	2.31

[a]Standard uncertainties: $u(x_1)$ = 0.0002, $u(x_2)$ = 0.0002, $u(T)$ = 0.1 K, $u(p)$ = 1 kPa, and the relative standard uncertainty is $u_r(\mu)$ = 0.15.

Table 8. Fitted Results for Viscosities of DGM, DMSO, TMS, MEA−DGM, DETA−DGM, DETA−TMS, MEA−TMS, and DETA−DMSO Aqueous Solutions

	k_1	k_2	k_3	k_4	k_5	k_6	AAD	R^2
DGM	9064.01	0.4522	1.07×10^8	-2.59×10^3	7.75×10^5	−239.09	9.27×10^{-3}	0.9982
TMS	−942.93	3.5477	2.79×10^6	-1.75×10^3	5.30×10^5	−7.50	1.91×10^{-2}	0.9909
DMSO	229.29	1.7476	4.66×10^6	-2.04×10^3	6.05×10^5	−12.68	5.73×10^{-3}	0.9987
MEA−DGM	215.68	31.191	1.43×10^3	-2.80×10^3	9.31×10^5	−0.04	2.76×10^{-3}	0.9982
DETA−DGM	4.13×10^7	0.7543	4.89×10^{10}	-8.44×10^3	1.82×10^6	−24.39	2.17×10^{-3}	0.9959
DETA−TMS	618.84	2.8813	7.55×10^5	-2.74×10^3	9.17×10^5	−1.35	6.68×10^{-3}	0.9996
MEA−TMS	339.42	7.6333	2.83×10^4	-2.43×10^3	7.96×10^5	−0.09	2.46×10^{-3}	0.9994
DETA−DMSO	527.51	3.9833	6.51×10^5	-2.85×10^3	9.53×10^5	−1.59	5.88×10^{-3}	0.9988

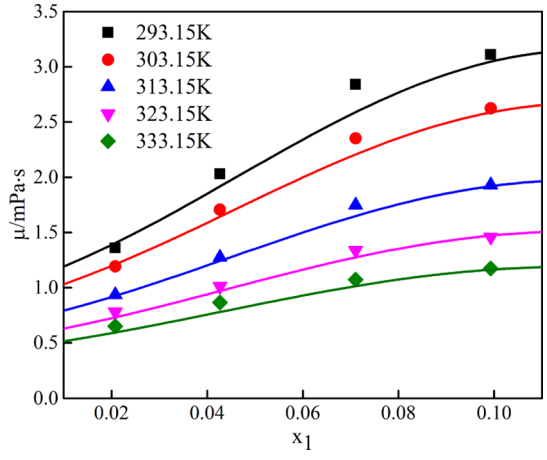

Figure 13. Viscosities of aqueous DGM solutions from this work. Solid lines, calculated in this work; markers, experimental data.

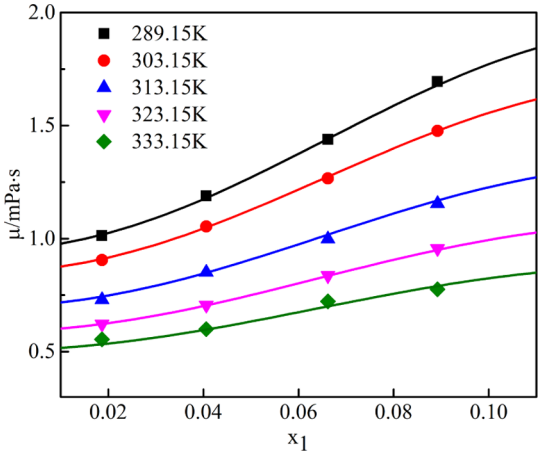

Figure 14. Viscosities of aqueous DMSO solutions from this work. Solid lines, calculated in this work; markers, experimental data.

and Table 9. As shown in Figures 21 and 22, the N_2O solubility in DETA−TMS/DGM and MEA−TMS/DGM increases with the increasing TMS or DGM concentration, while decreases with the increase of DMSO concentration in DMSO−DETA solution.

https://dx.doi.org/10.1021/acs.jced.9b00806
J. Chem. Eng. Data 2020, 65, 598−608

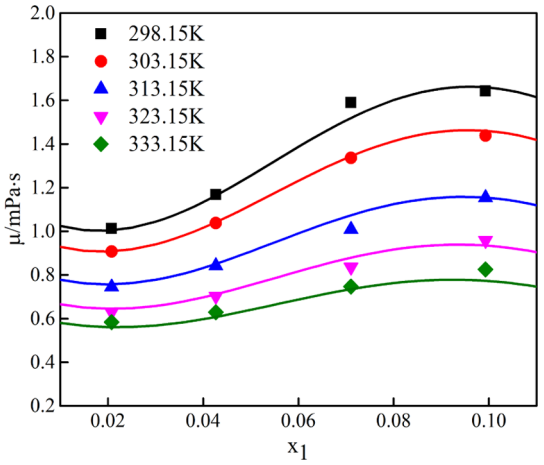

Figure 15. Viscosities of aqueous TMS solutions from this work. Solid lines, calculated in this work; markers, experimental data.

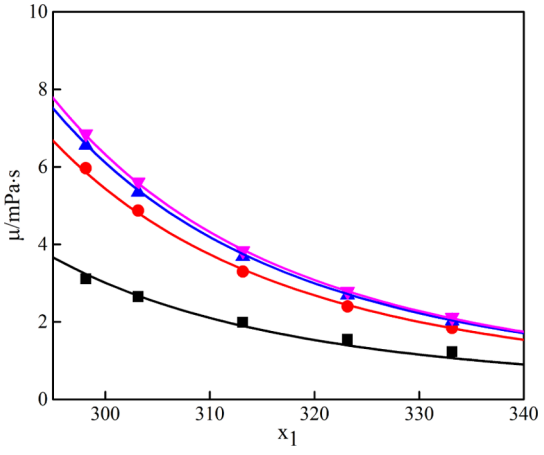

Figure 16. Viscosity results of aqueous MEA−DGM solutions in this work. The $10x_1/10x_2$ (mol/mol) are 1.422/0, 1.831/0.455, 2.045/0.682, and 2.312/0.963 for black ■, red ●, blue ▲, and pink ▼, respectively. Solid lines, calculated in this work.

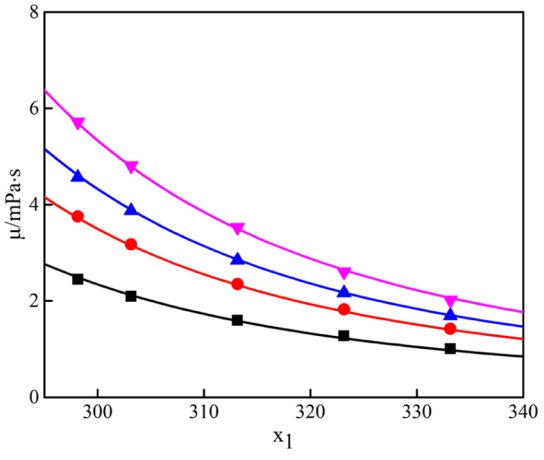

Figure 17. Viscosities of aqueous MEA−TMS solutions measured and calculated in this work. The $10x_1/10x_2$ (mol/mol) are 1.121/0, 1.390/0.554, 1.578/0.944, and 1.821/1.457 for black ■, red ●, blue ▲, and pink ▼, respectively. Solid lines, calculated in this work.

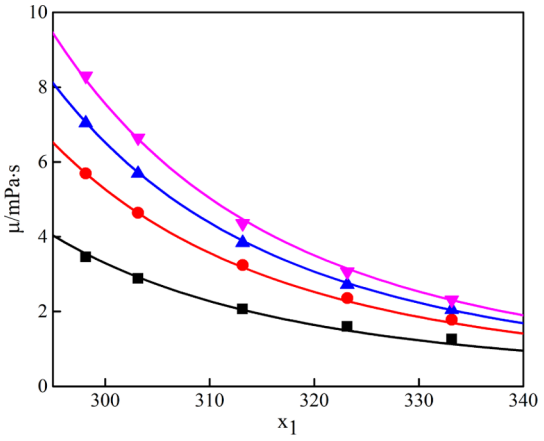

Figure 18. Viscosities of aqueous DETA−DMSO solutions measured and calculated in this work. The $10x_1/10x_2$ (mol/mol) are 0.568/0, 0.642/0.519, 0.688/0.826, and 0.742/1.187 for black ■, red ●, blue ▲, and pink ▼, respectively. Solid lines, calculated in this work.

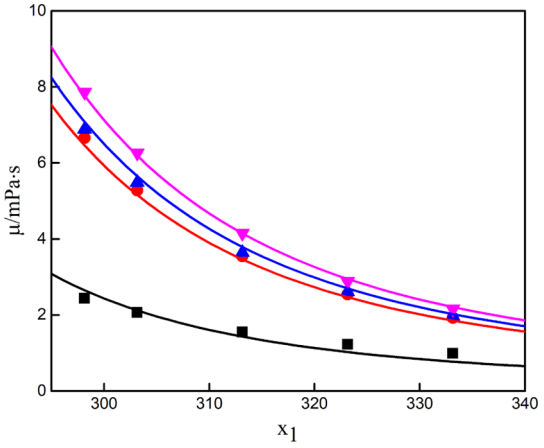

Figure 19. Viscosities of aqueous DETA−DGM solutions measured and calculated in this work. The $10x_1/10x_2$ (mol/mol) are 0.425/0, 0.604/0.627, 0.637/0.795, and 0.726/1.088 for black ■, red ●, blue ▲, and pink ▼, respectively. Solid lines, calculated in this work.

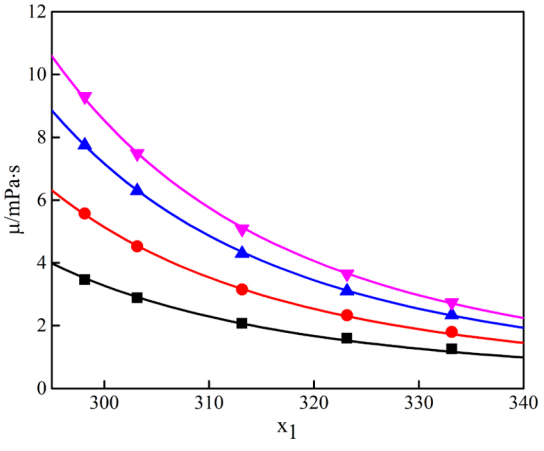

Figure 20. Viscosities of aqueous DETA−TMS solutions measured and calculated in this work. The $10x_1/10x_2$ (mol/mol) are 0.568/0, 0.696/0.560, 0.813/1.061, and 0.906/1.449 for black ■, red ●, blue ▲, and pink ▼, respectively. Solid lines, calculated in this work.

Equation 9 was used to fit the experimental data, the temperature and the mole fractions of amines and physical solvents are independent variables.[38] The fitted results (k_1−k_6, AADs, R^2) are given in Table 10, which shows that eq 9 gives

https://dx.doi.org/10.1021/acs.jced.9b00806
J. Chem. Eng. Data 2020, 65, 598−608

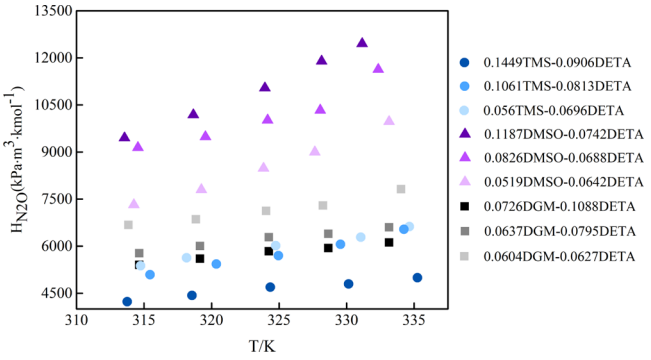

Figure 21. N_2O solubility H_{N_2O} in aqueous DETA−TMS/DMSO/DGM solutions measured in this work.

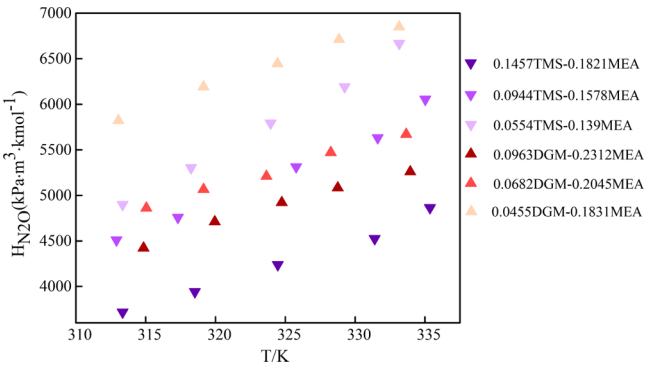

Figure 22. N_2O solubility H_{N_2O} in aqueous MEA−DGM/TMS solutions measured in this work.

reasonable results consistent with the experimental results in this work with an AAD less than 0.53%.

$$H_{N_2O} = \left(1 + \frac{k_1 x_1}{T} + \frac{k_2 x_2}{T^2}\right)\exp\left[\frac{k_3}{T} + \frac{k_4}{T^2} + k_5\left(\frac{x_1 x_2}{T}\right)^2\right] \quad (9)$$

where H_{N_2O} is the Henry's law constant, Pa·m^3·mol^{-1}; T is temperature, K; x_1 and x_2 are the mole fraction of amines and physical solvents, respectively; and k_1−k_5 are the correlation parameters.

4. CONCLUSIONS

Physicochemical properties of aqueous MEA−DGM, DETA−DGM, DETA−TMS, MEA−TMS, and DETA−DMSO solutions and their phase separation accelerators DGM, DMSO, and TMS solution were studied. The experiments cover the mole fraction ranges (0−13.5 mol %) DGM, (0−8.92 mol %) DMSO, (0−9.93 mol %) TMS, (14.22−23.12 mol %) MEA + (0−9.63 mol %) DGM, (4.25−7.26 mol %) DETA + (0−10.88 mol %) DGM, (5.68−9.06 mol %) DETA + (0−14.49 mol %) TMS, (11.21−18.21 mol %) MEA + (0−14.57 mol %) TMS, and (5.68−7.42 mol %) DETA + (0−11.87 mol %) DMSO in the blended solutions. Densities and viscosities were measured from 293.15 to 333.15 K and the Henry's constant of N_2O in blends was studied from 313.15 to 333.15 K. Empirical equations were used to fit the experimental results, and the physical parameters can be calculated by the temperature and mole fractions of amines and physical solvents within a high correlation coefficient. In ternary solution, densities decrease faster with increasing temperature when adding DGM to MEA and DETA solution, while densities increase with the addition of

Table 9. Henry's Law Constant H of N_2O in MEA−DGM, DETA−DGM, DETA−TMS, MEA−TMS, and DETA−DMSO (Mole Fraction of Amines x_1, Mole Fraction of Physical Solvents x_2) Aqueous Solutions[a]

	H_{N_2O} (kPa·m^3·kmol^{-1})							
	$10x_1/10x_2$ (mol/mol)							
	1.121/0		1.390/0.554		1.578/0.944		1.821/1.457	
	T/K	H	T/K	H	T/K	H	T/K	H
MEA−TMS	303.15	5144	333.15	6667	332.75	6054	333.05	4864
	313.15	5673	329.25	6192	329.65	5632	329.45	4525
	319.75	7037	323.95	5793	324.35	5312	323.15	4238
	328.25	8066	318.25	5302	316.65	4757	317.75	3942
	337.75	9235	313.35	4898	312.65	4509	313.05	3717
	H_{N_2O} (kPa·m^3·kmol^{-1})							
	$10x_1/10x_2$ (mol/mol)							
	0.568/0		0.696/0.560		0.813/1.061		0.906/1.449	
	T/K	H	T/K	H	T/K	H	T/K	H
DETA−TMS	333.75	10,278	334.65	6624	334.25	6535	335.25	4992
	328.85	9538	331.05	6283	329.55	6060	330.15	4796
	324.25	8971	324.75	6013	324.95	5698	324.35	4692
	319.35	8208	318.15	5626	320.35	5429	318.55	4428
	313.65	7251	314.75	5377	315.45	5088	313.75	4229
	H_{N_2O} (kPa·m^3·kmol^{-1})							
	$10x_1/10x_2$ (mol/mol)							
	0.568/0		0.642/0.519		0.688/0.826		0.742/1.187	
	T/K	H	T/K	H	T/K	H	T/K	H
DETA−DMSO	333.75	10,278	333.15	9969	332.35	11,629	331.15	12,450
	328.85	9538	327.65	8999	328.05	10,331	328.15	11,893
	324.25	8971	323.85	8480	324.15	10,013	323.95	11,039

https://dx.doi.org/10.1021/acs.jced.9b00806
J. Chem. Eng. Data 2020, 65, 598−608

Table 9. continued

	H_{N_2O} (kPa·m^3·kmol^{-1}) $10x_1/10x_2$ (mol/mol)							
	0.568/0		0.642/0.519		0.688/0.826		0.742/1.187	
	T/K	H	T/K	H	T/K	H	T/K	H
	319.35	8208	319.25	7799	319.55	9485	318.65	10,184
	313.65	7251	313.15	7415	314.55	9139	313.55	9447
	H_{N_2O} (kPa·m^3·kmol^{-1}) $10x_1/10x_2$ (mol/mol)							
	0.425/0		0.604/0.627		0.637/0.795		0.726/1.088	
	T/K	H	T/K	H	T/K	H	T/K	H
DETA−DGM	333.35	9254	334.05	7814	333.15	6600	333.15	6116
	328.95	8912	328.25	7294	328.65	6390	328.65	5935
	324.55	8370	324.05	7118	324.25	6279	324.25	5835
	320.05	7719	318.85	6852	319.15	6002	319.15	5598
	315.65	7139	313.85	6673	314.65	5770	314.65	5397
	H_{N_2O} (kPa·m^3·kmol^{-1}) $10x_1/10x_2$ (mol/mol)							
	1.422/0		1.831/0.455		2.045/0.682		2.312/0.963	
	T/K	H	T/K	H	T/K	H	T/K	H
MEA−DGM	333.15	7903	333.15	6850	333.65	5670	333.95	5260
	328.85	7708	328.85	6710	328.25	5470	328.75	5083
	324.55	7431	324.45	6446	323.65	5210	324.75	4921
	319.45	6955	319.15	6192	319.15	5065	319.95	4710
	315.45	6512	313.05	5822	315.05	4860	314.85	4422

[a]Standard uncertainties: $u(x_1)$ = 0.0002, $u(x_2)$ = 0.0002, $u(T)$ = 0.1 K, $u(p)$ = 1 kPa, and the expanded uncertainty is $U(H)$ = 48 Pa·m^3·mol^{-1} (0.95 level of confidence).

Table 10. Fitted Results for H_{N_2O} of MEA−DGM, DETA−DGM, DETA−TMS, MEA−TMS, and DETA−DMSO Solutions

	k_1	k_2	k_3	k_4	k_5	AAD	R^2
MEA−TMS	1.335×10^{10}	-3.883×10^{12}	-2.270×10^{3}	5.863×10^{4}	3.706×10^{7}	3.231×10^{-3}	0.9484
DETA−TMS	4.758×10^{9}	-8.240×10^{9}	-2.061×10^{3}	1.333×10^{5}	-3.464×10^{8}	3.609×10^{-5}	0.9694
DETA−DMSO	7.205×10^{15}	1.540×10^{18}	-1.053×10^{4}	1.383×10^{6}	-2.725×10^{8}	-5.267×10^{-3}	0.9868
DETA−DGM	7.498×10^{8}	-1.159×10^{11}	-8.580×10^{2}	3.173×10^{4}	3.862×10^{8}	-9.909×10^{-4}	0.9727
MEA−DGM	1.211×10^{6}	-7.157×10^{8}	2.573×10^{3}	-5.434×10^{5}	7.724×10^{7}	-9.177×10^{-4}	0.9254

TMS or DMSO to DETA or MEA solutions at the same temperature. The viscosities of binary and ternary blends go up with the increase of the physical solvent mole fraction or the decrease of temperature. The N_2O solubility in biphasic solvents increases with the increasing mole fraction of TMS and DGM or with the decreasing concentration of DMSO.

■ ASSOCIATED CONTENT

Supporting Information

The Supporting Information is available free of charge at https://pubs.acs.org/doi/10.1021/acs.jced.9b00806.

Experimental data and the uncertainty calculation equations (PDF)

■ AUTHOR INFORMATION

Corresponding Author

Shujuan Wang − *Tsinghua University, Beijing, China*; Email: wangshuj@tsinghua.edu.cn

Other Authors

Mimi Xu − *Tsinghua University, Beijing, China*; orcid.org/0000-0002-2202-3014

Lizhen Xu − *Tsinghua University, Beijing, China*

Complete contact information is available at: https://pubs.acs.org/10.1021/acs.jced.9b00806

Notes

The authors declare no competing financial interest.

■ ACKNOWLEDGMENTS

This work is financially supported by National Key R&D Program of China (2017YFB0603301).

■ REFERENCES

(1) Rochelle, G. T. Amine scrubbing for CO_2 capture. *Science* **2009**, *325*, 1652−1654.

(2) Bishnoi, S.; Rochelle, G. T. Absorption of carbon dioxide in aqueous piperazine/methyldiethanolamine. *AIChE J.* **2002**, *48*, 2788−2799.

(3) Mandal, B. P.; Biswas, A. K.; Bandyopadhyay, S. S. Absorption of carbon dioxide into aqueous blends of 2-amino-2-methyl-1-propanol and diethanolamine. *Chem. Eng. Sci.* **2003**, *58*, 4137−4144.

(4) Zhao, B.; Liu, F.; Cui, Z.; Liu, C.; Yue, H.; Tang, S.; Liu, Y.; Lu, H.; Liang, B. Enhancing the energetic efficiency of MDEA/PZ-based CO_2

capture technology for a 650 MW power plant: process improvement. *Appl. Energy* **2017**, *185*, 362−375.
(5) Pinto, D. D. D.; Knuutila, H.; Fytianos, G.; Haugen, G.; Mejdell, T.; Svendsen, H. F. CO_2 post combustion capture with a phase change solvent. Pilot plant campaign. *Int. J. Greenhouse Gas Control* **2014**, *31*, 153−164.
(6) Raynal, L.; Alix, P.; Bouillon, P.-A.; Gomez, A.; de Nailly, M. l. F.; Jacquin, M.; Kittel, J.; di Lella, A.; Mougin, P.; Trapy, J. The DMX process: an original solution for lowering the cost of post-combustion carbon capture. *Energy Procedia* **2011**, *4*, 779−786.
(7) Xu, Z.; Wang, S.; Chen, C. Solubility of N_2O in and Density and Viscosity of Aqueous Solutions of 1,4-Butanediamine, 2-(Diethylamino)-ethanol, and Their Mixtures from (298.15 to 333.15) K. *J. Chem. Eng. Data* **2013**, *58*, 1633−1640.
(8) Ciftja, A. F.; Hartono, A.; Svendsen, H. F. Experimental study on phase change solvents in CO_2 capture by NMR spectroscopy. *Chem. Eng. Sci.* **2013**, *102*, 378−386.
(9) Ye, Q.; Wang, X.; Lu, Y. Screening and evaluation of novel biphasic solvents for energy-efficient post-combustion CO_2 capture. *Int. J. Greenhouse Gas Control* **2015**, *39*, 205−214.
(10) Zhang, S.; Shen, Y.; Shao, P.; Chen, J.; Wang, L. Kinetics, Thermodynamics, and Mechanism of a Novel Biphasic Solvent for CO_2 Capture from Flue Gas. *Environ. Sci. Technol.* **2018**, *52*, 3660−3668.
(11) Xu, M.; Wang, S.; Xu, L. Screening of physical-chemical biphasic solvents for CO_2 absorption. *Int. J. Greenhouse Gas Control* **2019**, *85*, 199−205.
(12) Dindore, V. Y.; Brilman, D. W. F.; Feron, P. H. M.; Versteeg, G. F. CO_2 absorption at elevated pressures using a hollow fiber membrane contactor. *J. Membr. Sci.* **2004**, *235*, 99−109.
(13) Clarke, J. K. A. Kinetics of absorption of cardon dioxide in monoethanolamine solutions at short contact times. *Ind. Eng. Chem. Fundam.* **1964**, *3*, 239−245.
(14) Laddha, S. S.; Diaz, J. M.; Danckwerts, P. V. The N_2O analogy: the solubilities of CO_2 and N_2O in aqueous solutions of organic compounds. *Chem. Eng. Sci.* **1981**, *36*, 228−229.
(15) Mandal, B. P.; Kundu, M.; Bandyopadhyay, S. S. Physical solubility and diffusivity of N2O and CO2 into aqueous solutions of (2-amino-2-methyl-1-propanol+ monoethanolamine) and (N-methyldiethanolamine+ monoethanolamine). *J. Chem. Eng. Data* **2005**, *50*, 352−358.
(16) Monteiro, J. G. M.-S.; Svendsen, H. F. The N_2O analogy in the CO_2 capture context: Literature review and thermodynamic modelling considerations. *Chem. Eng. Sci.* **2015**, *126*, 455−470.
(17) Hartono, A.; Svendsen, H. F. Density, viscosity, and excess properties of aqueous solution of diethylenetriamine (DETA). *J. Chem. Thermodyn.* **2009**, *41*, 973−979.
(18) Li, M. H.; Shen, K. P. Densities and solubilities of solutions of carbon dioxide in water + monoethanolamine + N-methyldiethanolamine. *J. Chem. Eng. Data* **1992**, *37*, 288−290.
(19) Xu, L.; Wang, S. Density, Viscosity, and N_2O Solubility of Aqueous Solutions of MEA, $BmimBF_4$, and Their Mixtures from 293.15 to 333.15 K. *J. Chem. Eng. Data* **2018**, *63*, 2708−2717.
(20) Xu, Q.; Sun, S.; Lan, G.; Xiao, J.; Zhang, J.; Wei, X. Excess properties and spectral investigation for the binary system diethylene glycol dimethyl ether+ water at T=(293.15, 298.15, 303.15, 308.15, and 313.15) K. *J. Chem. Eng. Data* **2015**, *60*, 2−10.
(21) Jalili, A. H.; Shokouhi, M.; Samani, F.; Hosseini-Jenab, M. Measuring the solubility of CO2 and H2S in sulfolane and the density and viscosity of saturated liquid binary mixtures of (sulfolane+ CO2) and (sulfolane+ H2S). *J. Chem. Thermodyn.* **2015**, *85*, 13−25.
(22) López, E. R.; Daridon, J. L.; Plantier, F.; Boned, C.; Fernández, J. Temperature and pressure dependences of thermophysical properties of some ethylene glycol dimethyl ethers from ultrasonic measurements. *Int. J. Thermophys.* **2006**, *27*, 1354−1372.
(23) Schichman, S. A.; Amey, R. L. Viscosity and local liquid structure in dimethyl sulfoxide-water mixtures. *J. Phys. Chem.* **1971**, *75*, 98−102.
(24) Comuñas, M. J. P.; Baylaucq, A.; Boned, C.; Fernández, J. Volumetric properties of monoethylene glycol dimethyl ether and diethylene glycol dimethyl ether up to 60 MPa. *J. Chem. Eng. Data* **2003**, *48*, 1044−1049.
(25) Wallace, W. J.; Mathews, A. L. Density, Refractive Indices, Molar Refractions, and Viscosities of Diethylene Glycol Dimethyl Ether-Water Solutions at 25 °C. *J. Chem. Eng. Data* **1964**, *9*, 267−268.
(26) Yin, Y.; Zhu, C.; Ma, Y. Volumetric and viscometric properties of binary and ternary mixtures of 1-butyl-3-methylimidazolium tetrafluoroborate, monoethanolamine and water. *J. Chem. Thermodyn.* **2016**, *102*, 413−428.
(27) Shoghl, S. N.; Jamali, J.; Moraveji, M. K. Electrical conductivity, viscosity, and density of different nanofluids: An experimental study. *Exp. Therm. Fluid Sci.* **2016**, *74*, 339−346.
(28) Song, J.-H.; Park, S.-B.; Yoon, J.-H.; Lee, H.; Lee, K.-H. Densities and Viscosities of Monoethanolamine + Ethylene Glycol + Water. *J. Chem. Eng. Data* **1996**, *41*, 1152−1154.
(29) Weast, R. C.; Astle, M. J.; Beyer, W. H. *CRC Handbook of Chemistry and Physics*; CRC Press: Boca Raton, FL, 1988; Vol. *69*.
(30) Li, M.-H.; Lie, Y.-C. Densities and Viscosities of Solutions of Monoethanolamine + N-methyldiethanolamine + Water and Monoethanolamine + 2-Amino-2-methyl-1-propanol + Water. *J. Chem. Eng. Data* **1994**, *39*, 444−447.
(31) Samanta, A.; Roy, S.; Bandyopadhyay, S. S. Physical Solubility and Diffusivity of N2O and CO2 in Aqueous Solutions of Piperazine and (N-Methyldiethanolamine + Piperazine). *J. Chem. Eng. Data* **2007**, *52*, 1381−1385.
(32) Versteeg, G. F.; Van Swaaij, W. P. M. Solubility and diffusivity of acid gases (carbon dioxide, nitrous oxide) in aqueous alkanolamine solutions. *J. Chem. Eng. Data* **1988**, *33*, 29−34.
(33) Jou, F.-Y.; Carroll, J. J.; Mather, A. E.; Otto, F. D. The solubility of nitrous oxide in water at high temperatures and pressures. *Z. Phys. Chem.* **1992**, *177*, 225−239.
(34) Saleh, M. A.; Shamsuddin Ahmed, M.; Begum, S. K. Density, viscosity and thermodynamic activation for viscous flow of water + sulfolane. *Phys. Chem. Liq.* **2006**, *44*, 153−165.
(35) Wang, Y.-W.; Otto, F. D.; Mather, A. E.; Xu, S. Solubilities and diffusivities of N2O and CO2 in aqueous sulfolane solutions. *J. Chem. Technol. Biotechnol.* **2007**, *51*, 197−208.
(36) Shokouhi, M.; Jalili, A. H.; Zoghi, A. T.; Sadeghzadeh Ahari, J. Carbon dioxide solubility in aqueous sulfolane solution. *J. Chem. Thermodyn.* **2019**, *132*, 62−72.
(37) Liu, J.; Wang, S.; Hartono, A.; Svendsen, H. F.; Chen, C. Solubility of N2O in and Density and Viscosity of Aqueous Solutions of Piperazine, Ammonia, and Their Mixtures from (283.15 to 323.15) K. *J. Chem. Eng. Data* **2012**, *57*, 2387−2393.
(38) Aronu, U. E.; Hartono, A.; Svendsen, H. F. Density, viscosity, and N_2O solubility of aqueous amino acid salt and amine amino acid salt solutions. *J. Chem. Thermodyn.* **2012**, *45*, 90−99.

https://dx.doi.org/10.1021/acs.jced.9b00806
J. Chem. Eng. Data 2020, 65, 598−608